

Application of Convolution of Daubechies Wavelet in Solving 3D Microscale DPL Problem

Zahra Kalateh Bojdi¹, Ataollah Askari Hemmat^{2*}, and Ali Tavakoli³

ABSTRACT. In this work, the triple convolution of Daubechies wavelet is used to solve the three dimensional (3D) microscale Dual Phase Lag (DPL) problem. Also, numerical solution of 3D time-dependent initial-boundary value problems of a microscopic heat equation is presented. To generate a 3D wavelet we used the triple convolution of a one dimensional wavelet. Using convolution we get a scaling function and a sevenfold 3D wavelet and all of our computations are based on this new set to approximate in 3D spatial. Moreover, approximation in time domain is based on finite difference method. By substitution in the 3D DPL model, the differential equation converts to a linear system of equations and related system is solved directly. We use the Lax-Richtmyer theorem to investigate the consistency, stability and convergence analysis of our method. Numerical results are presented and compared with the analytical solution to show the efficiency of the method.

1. INTRODUCTION

An applicable version of traditional heat equation is the microscopic heat flux equation, developed from physical and mathematical reasoning. Microscale heat transfer occurs in many physical phenomena like microchip [14], mobile phones and processing of materials [26]. The DPL heat conduction equation arises in many branches of physics and engineering, see [13, 19, 25]. Qui and Tien deduced a partial differential equation (PDE) model for the heat transfer in microscale [22, 23]. Recently a similar equation to energy equation without containing the electron energy storage is suggested [6, 25]. Several techniques have

2010 *Mathematics Subject Classification.* 65T60, 35Q79.

Key words and phrases. MRA, Heat equation, Wavelet method, Finite difference.

Received: 03 November 2017, Accepted: 06 March 2018.

* Corresponding author.

been used to obtain the numerical or analytical solutions of heat transfer problems [5, 27]. For solving the heat flux equation at microscale, finite difference methods used in one dimension [8, 10] and three dimensions [9, 11, 28]. Dai applied a higher-order accurate and unconditionally stable compact finite difference scheme for solving the DPL equation with the temperature jump boundary condition [7]. Malek and Kalateh Bojdi, investigated numerical solution of laser heating of nanoscale thin-films in three dimensions using DPL model based on mixed collocation-finite difference method [18]. Also Kargar and Saeedi, used B-spline wavelet operational method for solving fractional partial differential equations [16]. In this paper we will investigate the numerical solution of the 3D heat equation at microscale. The wavelet method is used to approximate the solution, and the finite difference scheme is used for time discretization. In Section 2 the DPL model is presented. MRA and wavelet method is presented in Section 3. In Section 4 the convergence of the method is investigated. In Section 5 numerical results and a comparison of numerical and analytical solutions are given.

2. DPL MODEL

The Fourier heat transfer law in the classical theory of diffusion is

$$(2.1) \quad q(r, t) = -\kappa \nabla U(r, t),$$

where κ is the conductivity, $q = (q_x, q_y, q_z)$ is the heat flux, r is the position vector that has heat flux components in the x , y and z directions, respectively, and U is the temperature. In Eq. (2.1), the heat flux q , and the temperature gradient ∇U are assumed to arise simultaneously. If one of the directions is at the microscale, (of order $0.1\mu m$), Tzou has shown that the temperature gradient and heat flux occur at different times in this direction and Eq. (2.1) has the following form (DPL model)[25]

$$(2.2) \quad q(r, t + \tau_q) = -\kappa \nabla U(r, t + \tau_U).$$

Also the heat conduction equation is given by [25]

$$(2.3) \quad -\nabla \cdot q + Q = \rho C_p \frac{\partial U}{\partial t},$$

where C_p is the specific heat, ρ is density, Q is a heat source, τ_q and τ_U are positive constants, which are the time lags of the heat flux and temperature gradient, respectively. Therefore, if the components of the heat flux in the z direction satisfy in Eq. (2.2), then

$$q_x(r, t) = -\kappa \frac{\partial U(r, t)}{\partial x},$$

$$q_y(r, t) = -\kappa \frac{\partial U(r, t)}{\partial y},$$

$$q_z(r, t + \tau_q) = -\kappa \frac{\partial U(r, t + \tau_U)}{\partial z}.$$

Using Taylor's expansion we have

$$(2.4) \quad q_z + \tau_q \frac{\partial q_z}{\partial t} = -\kappa \left(\frac{\partial U}{\partial z} + \tau_U \frac{\partial}{\partial t} \left(\frac{\partial U}{\partial z} \right) \right).$$

Differentiating the Eq. (2.4), and substituting the expression of $\nabla \cdot q$ in Eq. (2.3), implies

$$(2.5) \quad \frac{\rho C_p}{\kappa} \left(\frac{\partial U}{\partial t} + \tau_q \frac{\partial^2 U}{\partial t^2} \right) = \nabla^2 U + \tau_q \frac{\partial}{\partial t} \left(\frac{\partial^2 U}{\partial x^2} + \frac{\partial^2 U}{\partial y^2} \right) \\ + \tau_U \frac{\partial^3 U}{\partial t \partial z^2} + \frac{Q + \tau_q \partial Q / \partial t}{\kappa}.$$

Let the real-valued functions f and g are given. Therefore, the initial conditions at $t = 0$ are

$$(2.6) \quad U(x, y, z, 0) = f(x, y, z), \\ \frac{\partial U}{\partial t}(x, y, z, 0) = g(x, y, z).$$

We also assume that the solution of the above initial value problem is smooth. We consider

$$\Omega = \{(x, y, z) \mid 0 \leq x \leq l_x, 0 \leq y \leq l_y, 0 \leq z \leq l_z\}.$$

3. 3D MRA AND WAVELET METHOD

A nested sequence of closed subspaces of $L^2(\mathbb{R})$, $\{V_j\}_{j \in \mathbb{Z}}$, is called an MRA for $L^2(\mathbb{R})$ with scaling function φ , if $\overline{\bigcup_{j \in \mathbb{Z}} V_j} = L^2(\mathbb{R})$, $\bigcap_{j \in \mathbb{Z}} V_j = \{0\}$, $f(\cdot) \in V_j$ iff $f(2^{-j}\cdot) \in V_0$ and there exists a function $\varphi \in V_0$ such that $\{\varphi(\cdot - k) : k \in \mathbb{Z}\}$ is an orthonormal basis for V_0 [12, 21].

We can write

$$(3.1) \quad V_1 = V_0 \oplus W_0,$$

where W_0 is the orthogonal complement of V_0 in V_1 and $\{\psi(\cdot - k) : k \in \mathbb{Z}\}$ is an orthonormal basis for W_0 . ψ is called the wavelet generated by $\{V_j\}_{j \in \mathbb{Z}}$. Any $u \in L^2(\mathbb{R})$ can be approximated with arbitrary precision by elements of V_j . One can use the above conditions to get the following corollary [12].

Corollary 3.1. *Let $\{V_j\}_{j \in \mathbb{Z}}$ be an MRA for $L^2(\mathbb{R})$ with scaling function φ .*

(a) *There exist coefficients $\{a_k\}_{k \in \mathbb{Z}}$ such that*

$$\varphi(x) = \sum_{k \in \mathbb{Z}} a_k \varphi(2x - k).$$

(b) *For any $j, k \in \mathbb{Z}$ define $\varphi_{jk}(x) = 2^{j/2} \varphi(2^j x - k)$. Then $\{\varphi_{jk}(x)\}_{k \in \mathbb{Z}}$ is an orthonormal basis for V_j .*

If $\{V_j\}_{j \in \mathbb{Z}}$ is an MRA for $L^2(\mathbb{R})$ with scaling function φ and wavelet ψ , then $\{V'_j = V_j \otimes V_j \otimes V_j\}_{j \in \mathbb{Z}}$ is an MRA of $L^2(\mathbb{R}^3)$. Using Eq. (3.1), one can easily show that

$$\begin{aligned} (3.2) \quad V'_1 &= V_1^{(x)} \otimes V_1^{(y)} \otimes V_1^{(z)} \\ &= (V_0^{(x)} \oplus W_0^{(x)}) \otimes (V_0^{(y)} \oplus W_0^{(y)}) \otimes (V_0^{(z)} \oplus W_0^{(z)}) \\ &= (V_0^{(x)} \otimes V_0^{(y)} \otimes V_0^{(z)}) \oplus (V_0^{(x)} \otimes V_0^{(y)} \otimes W_0^{(z)}) \\ &\quad \oplus (V_0^{(x)} \otimes W_0^{(y)} \otimes V_0^{(z)}) \oplus (V_0^{(x)} \otimes W_0^{(y)} \otimes W_0^{(z)}) \\ &\quad \oplus (W_0^{(x)} \otimes V_0^{(y)} \otimes V_0^{(z)}) \oplus (W_0^{(x)} \otimes V_0^{(y)} \otimes W_0^{(z)}) \\ &\quad \oplus (W_0^{(x)} \otimes W_0^{(y)} \otimes V_0^{(z)}) \oplus (W_0^{(x)} \otimes W_0^{(y)} \otimes W_0^{(z)}) \\ &= V'_0 \oplus W_0'^1 \oplus W_0'^2 \oplus W_0'^3 \oplus W_0'^4 \oplus W_0'^5 \oplus W_0'^6 \oplus W_0'^7. \end{aligned}$$

In a similar way, one can compute every V'_j . This 3D multiresolution analysis requires one scaling function

$$\Phi(x, y, z) = \varphi(x)\varphi(y)\varphi(z) \in V'_0,$$

and seven wavelets

$$\begin{aligned} \Psi^1(x, y, z) &= \varphi(x)\varphi(y)\psi(z), & \Psi^2(x, y, z) &= \varphi(x)\psi(y)\varphi(z), \\ \Psi^3(x, y, z) &= \varphi(x)\psi(y)\psi(z), & \Psi^4(x, y, z) &= \psi(x)\varphi(y)\varphi(z), \\ \Psi^5(x, y, z) &= \psi(x)\varphi(y)\psi(z), & \Psi^6(x, y, z) &= \psi(x)\psi(y)\varphi(z), \\ \Psi^7(x, y, z) &= \psi(x)\psi(y)\psi(z), \end{aligned}$$

where Ψ^i is the wavelet associated to W'^i for $i = 1, 2, \dots, 7$, respectively.

Let φ be the scaling function of a Daubechies wavelet. Then there exists a sequence $\{a_k\}$ (the filter coefficients) such that [12]

$$(3.3) \quad \varphi(x) = \sum_{k=0}^{N-1} a_k \varphi(2x - k),$$

where N is an even positive integer and φ has compact support

$$\text{supp}(\varphi) \subset [0, N - 1].$$

Let $\varphi(x)$ be normalized, i.e. $\int_{-\infty}^{\infty} \varphi(x) dx = 1$. We now define autocorrelation function of φ by [2]

$$(3.4) \quad \theta(x) := (\varphi * \varphi(-\cdot))(x).$$

For $j \in \mathbb{Z}$, define $V_j = \overline{\text{span}} \{2^{j/2}\theta(2^j \cdot -k), k \in \mathbb{Z}\}$, then $\{V_j\}_{j \in \mathbb{Z}}$ generates an MRA with the scaling function θ , [12, 15]. Due to the orthonormality property of the set $\{\varphi(\cdot - n), n \in \mathbb{Z}\}$, the function θ satisfies

$$\theta(0) = \int \varphi(x)\varphi(x) dx = 1, \quad \theta(n) = \int \varphi(x)\varphi(x-n) dx = 0, \quad n \neq 0.$$

The function θ defined by Eq. (3.4) is $\theta(x) = \int \varphi(t)\varphi(t-x) dt$, and one can simply compute its second derivative, $\theta''(l) = -\int \varphi'(t)\varphi'(t-l) dt$. Define

$$\Gamma_l = \int \varphi'(t)\varphi'(t-l) dt.$$

Since φ has compact support on $[0, N-1]$, we have

$$\Gamma_{-l} = \Gamma_l, \quad \theta''(l) = -\Gamma_l, \quad |l| \leq N-2.$$

MATLAB software is used to compute Γ [1, 15, 17]. Thus we compute second derivative of the function θ at the points $x_l = l2^{-j}$.

3.1. 3D Wavelet Method. Let j_x, j_y and j_z be arbitrary natural numbers. We can estimate the solution of Eq. (5.3) with corresponding initial conditions at a fixed time level by

$$(3.5) \quad \begin{aligned} U(\xi, \eta, \zeta, t) &\simeq U_{j_x, j_y, j_z}(\xi, \eta, \zeta, t) \\ &= \sum_{i=0}^{l_x} \sum_{j=0}^{l_y} \sum_{k=0}^{l_z} U_{ijk}(t) \Theta_{i,j,k}(\xi, \eta, \zeta), \end{aligned}$$

where $U_{ijk}(t) = U(\xi_i, \eta_j, \zeta_k, t)$ and

$$\Theta_{i,j,k}(\xi, \eta, \zeta) = \theta(2^{j_x}\xi - i) \theta(2^{j_y}\eta - j) \theta(2^{j_z}\zeta - k).$$

Thus the discretization of Eq. (5.3) at given collocation points $\xi_i = i2^{-j_x}$, $\eta_j = j2^{-j_y}$ and $\zeta_k = k2^{-j_z}$, is

$$(3.6) \quad \begin{aligned} &-2^{2j_x} \sum_{i=0}^{l_x} U_{ipl} \Gamma_{m-i} - 2^{2j_y} \sum_{j=0}^{l_y} U_{mjl} \Gamma_{p-j} - 2^{2j_z} \sum_{k=0}^{l_z} U_{mpk} \Gamma_{l-k} \\ &- \tau_U 2^{2j_z} \frac{\partial}{\partial t} \left(\sum_{k=0}^{l_z} U_{mpk} \Gamma_{l-k} \right) + \tau_q \frac{\partial}{\partial t} \left[-2^{2j_x} \sum_{i=0}^{l_x} U_{ipl} \Gamma_{m-i} - 2^{2j_y} \sum_{j=0}^{l_y} U_{mjl} \Gamma_{p-j} \right] \\ &= \frac{\rho C_p}{\kappa} \left(\frac{\partial U}{\partial t} + \tau_q \frac{\partial^2 U}{\partial t^2} \right) - \frac{Q + \tau_q \partial Q / \partial t}{\kappa}, \end{aligned}$$

for $m = 0, 1, \dots, l_x$, $p = 0, 1, \dots, l_y$ and $l = 0, 1, \dots, l_z$. The derivatives of U are estimated

$$(3.7) \quad \frac{\partial U}{\partial t} \simeq \frac{U^{n+1} - U^n}{\Delta t}, \quad \frac{\partial^2 U}{\partial t^2} \simeq \frac{U^{n-1} - 2U^n + U^{n+1}}{\Delta t^2}.$$

Therefore, from Eq. (3.6), we can write

$$(3.8) \quad \begin{aligned} & \frac{\tau_q}{\Delta t} 2^{2j_x} \sum_{i=0}^{l_x} U_{ipl}^{n+1} \Gamma_{m-i} + \frac{\tau_q}{\Delta t} 2^{2j_y} \sum_{j=0}^{l_y} U_{mjl}^{n+1} \Gamma_{p-j} \\ & + \frac{\tau_U}{\Delta t} 2^{2j_z} \sum_{k=0}^{l_z} U_{mpk}^{n+1} \Gamma_{l-k} + \frac{(\Delta t + \tau_q)}{\alpha (\Delta t)^2} U_{mpl}^{n+1} \\ & = \left(\frac{\tau_q}{\Delta t} - 1 \right) 2^{2j_x} \sum_{i=0}^{l_x} U_{ipl}^n \Gamma_{m-i} + \left(\frac{\tau_q}{\Delta t} - 1 \right) 2^{2j_y} \sum_{j=0}^{l_y} U_{mjl}^n \Gamma_{p-j} \\ & + \left(\frac{\tau_U}{\Delta t} - 1 \right) 2^{2j_z} \sum_{k=0}^{l_z} U_{mpk}^n \Gamma_{l-k} + \frac{(\Delta t + 2\tau_q)}{\alpha (\Delta t)^2} U_{mpl}^n \\ & - \frac{\tau_q}{\alpha (\Delta t)^2} U_{mpl}^{n-1} + \left(\frac{Q + \tau_q \partial Q / \partial t}{\kappa} \right)_{mpl}^n, \end{aligned}$$

for $n = 0, 1, 2, \dots$, where $\alpha = \frac{\kappa}{\rho C_p}$. Now, the system will be

$$(3.9) \quad AU^{n+1} = BU^n + CU^{n-1} + D^n,$$

where

$$C = -\frac{\tau_q}{\alpha (\Delta t)^2},$$

is a scalar and the vector D^n is generated by the boundary conditions and source terms.

4. THE CONVERGENCE OF THE METHOD

In this section, we will show that the proposed method is convergent. To do this, we need the following theorem, that is known as the Lax-Richtmyer theorem [4, 24].

Theorem 4.1. *A consistent finite-difference scheme for a partial differential equation for which the initial-value problem is well posed is convergent if and only if it is stable.*

Thus we will prove that our scheme is consistent and stable.

Let $P(U_{mpl})$ illustrate the PDE operator of Eq. (3.6) at fixed collocation point (x_m, y_p, z_l) and independent variable t with exact solution

U_{mpl} . Moreover, let $P^n(U_{mpl})$ represent the approximating wavelet-finite difference operator with exact solution U_{mpl} for a fixed time-level associated to Eq. (3.8). Suppose V_{mpl} is a continuous function of t with a sufficient number of continuous derivatives to enable $P(V_{mpl})$ to be evaluated at point $n\Delta t$. Then the truncation error $E^n(V_{mpl})$ for all $m = 0, 1, \dots, l_x$, $p = 0, 1, \dots, l_y$, $l = 0, 1, \dots, l_z$, at the point $n\Delta t$, is given by

$$(4.1) \quad E^n(V_{mpl}) = P^n(V_{mpl}) - P(V_{mpl}^n),$$

where $V_{mpl}^n = V_{mpl}(n\Delta t)$.

If $E^n(V_{mpl})$ tends to zero as Δt tends to zero, then the Eq. (3.8) is consistent with the PDE (3.6), [24]. In the following, we show that the truncation error $E^n(V_{mpl})$ is $O(\Delta t)$.

By expanding U_{mpl}^{n+1} and U_{mpl}^n in Eq. (3.8) at the point $(x_m, y_p, z_l, n\Delta t) \in \Omega \times [0, T]$, we have

$$(4.2) \quad \begin{aligned} & \frac{\tau_q}{\Delta t} 2^{2j_x} \sum_{i=0}^{l_x} \left[U_{ipl}^n + \Delta t \left(\frac{\partial U}{\partial t} \right)_{ipl}^n + \frac{(\Delta t)^2}{2} \left(\frac{\partial^2 U}{\partial t^2} \right)_{ipl}^n + O((\Delta t)^3) \right] \Gamma_{m-i} \\ & + \frac{\tau_q}{\Delta t} 2^{2j_y} \sum_{j=0}^{l_y} \left[U_{mjl}^n + \Delta t \left(\frac{\partial U}{\partial t} \right)_{mjl}^n + \frac{(\Delta t)^2}{2} \left(\frac{\partial^2 U}{\partial t^2} \right)_{mjl}^n + O((\Delta t)^3) \right] \Gamma_{p-j} \\ & + \frac{\tau_U}{\Delta t} 2^{2j_z} \sum_{k=0}^{l_z} \left[U_{mpk}^n + \Delta t \left(\frac{\partial U}{\partial t} \right)_{mpk}^n + \frac{(\Delta t)^2}{2} \left(\frac{\partial^2 U}{\partial t^2} \right)_{mpk}^n + O((\Delta t)^3) \right] \Gamma_{l-k}(\zeta_l) \\ & + \frac{\Delta t + \tau_q}{\alpha (\Delta t)^2} \left[U_{mpl}^n + \Delta t \left(\frac{\partial U}{\partial t} \right)_{mpl}^n + \frac{(\Delta t)^2}{2} \left(\frac{\partial^2 U}{\partial t^2} \right)_{mpl}^n + O((\Delta t)^3) \right] \\ & = -\frac{\tau_q}{\alpha (\Delta t)^2} \left[U_{mpl}^n - \Delta t \left(\frac{\partial U}{\partial t} \right)_{mpl}^n + \frac{(\Delta t)^2}{2} \left(\frac{\partial^2 U}{\partial t^2} \right)_{mpl}^n + O((\Delta t)^3) \right] \\ & + \left(\frac{\tau_q}{\Delta t} - 1 \right) 2^{2j_x} \sum_{i=0}^{l_x} U_{ipl}^n \Gamma_{m-i} + \left(\frac{\tau_q}{\Delta t} - 1 \right) 2^{2j_y} \sum_{j=0}^{l_y} U_{mjl}^n \Gamma_{p-j} \\ & + \left(\frac{\tau_U}{\Delta t} - 1 \right) 2^{2j_z} \sum_{k=0}^{l_z} U_{mpk}^n \Gamma_{l-k} + \frac{\Delta t + 2\tau_q}{\alpha (\Delta t)^2} U_{mpl}^n + \left(\frac{Q + \tau_q \partial Q / \partial t}{\kappa} \right)_{mpl}^n, \end{aligned}$$

for $n = 0, 1, 2, \dots$, $m = 0, 1, \dots, l_x$, $p = 0, 1, \dots, l_y$ and $l = 0, 1, \dots, l_z$. From Eq. (3.6) we can write

$$(4.3) \quad -2^{2j_x} \sum_{i=0}^{l_x} U_{ipl}^n \Gamma_{m-i} - 2^{2j_y} \sum_{j=0}^{l_y} U_{mjl}^n \Gamma_{p-j} - 2^{2j_z} \sum_{k=0}^{l_z} U_{mpk}^n \Gamma_{l-k}$$

$$\begin{aligned}
& -\tau_q \left[2^{2j_x} \sum_{i=0}^{l_x} \left(\frac{\partial U}{\partial t} \right)_{ipl}^n \Gamma_{m-i} + 2^{2j_y} \sum_{j=0}^{l_y} \left(\frac{\partial U}{\partial t} \right)_{mjl}^n \Gamma_{p-j} \right] \\
& - 2^{2j_z} \tau_U \sum_{k=0}^{l_z} \left(\frac{\partial U}{\partial t} \right)_{mpk}^n \Gamma_{l-k} \\
& = \frac{\rho C_p}{\kappa} \left(\frac{\partial U}{\partial t} \right)_{mpl}^n + \frac{\rho C_p \tau_q}{\kappa} \left(\frac{\partial^2 U}{\partial t^2} \right)_{mpl}^n \\
& - \left(\frac{Q + \tau_q \partial Q / \partial t}{\kappa} \right)_{mpl}^n.
\end{aligned}$$

Hence the truncated error will be found from subtracting Eqs. (4.2) and (4.3), i.e.,

(4.4)

$$\begin{aligned}
E^n(U_{mpl}) &= \tau_q \frac{\Delta t}{2} \left[2^{2j_x} \sum_{i=0}^{l_x} \left(\frac{\partial^2 U}{\partial t^2} \right)_{ipl}^n \Gamma_{m-i} + 2^{2j_y} \sum_{j=0}^{l_y} \left(\frac{\partial^2 U}{\partial t^2} \right)_{mjl}^n \Gamma_{p-j} \right] \\
& + \tau_U \frac{\Delta t}{2} 2^{2j_z} \sum_{k=0}^{l_z} \left(\frac{\partial^2 U}{\partial t^2} \right)_{mpk}^n \Gamma_{l-k} + \frac{\Delta t}{2\alpha} \left(\frac{\partial^2 U}{\partial t^2} \right)_{mpl}^n + O(\Delta t).
\end{aligned}$$

Clearly $E^n(U_{mpl})$ vanishes as Δt tends to zero and l_x , l_y and l_z tend to infinity [3].

Eq. (3.9) can be represented as following (see [20])

$$(4.5) \quad F^{n+1} = W_N F^n + E^n, \quad n = 1, 2, \dots,$$

where

$$F^n = \begin{bmatrix} U_N^n \\ U_N^{n-1} \end{bmatrix}, \quad W_N = \begin{bmatrix} A_N^{-1} B_N & A_N^{-1} C_N \\ I_N & 0 \end{bmatrix}, \quad E^n = \begin{bmatrix} A_N^{-1} D_N^n \\ 0 \end{bmatrix}.$$

If each eigenvalue of W_N has a modulus ≤ 1 , i.e., $\rho(W_N) \leq 1$, we say Eq. (4.5) is stable. The eigenvalues of W_N can be evaluated numerically [24].

Therefore by the Lax-Richtmyer Theorem, the scheme is convergent.

5. NUMERICAL RESULTS

Example 5.1. Suppose $\frac{\rho C_p}{\kappa} = 1$, $\tau_q = \frac{1}{\pi^2} + 10^3$, $\tau_U = \frac{1}{\pi^2} - 1.99 \times 10^{-5}$, $Q = 0$, $0 \leq x, y \leq 0.1$ mm, $0 \leq z \leq 10^{-5}$ mm, where the initial and boundary conditions are

$$\begin{aligned}
U(x, y, z, 0) &= \cos(10\pi x) \sin(10\pi y) \cos(10^5 \pi z), \\
\frac{\partial U}{\partial t}(x, y, z, 0) &= -\pi^2 \cos(10\pi x) \sin(10\pi y) \cos(10^5 \pi z),
\end{aligned}$$

$$U(0, y, z, t) = -U(0.1, y, z, t) = \exp(-\pi^2 t) \sin(10\pi y) \cos(10^5 \pi z),$$

$$U(x, 0, z, t) = U(x, 0.1, z, t) = 0,$$

$$U(x, y, 0, t) = -U(x, y, 0.1, t) = \exp(-\pi^2 t) \cos(10\pi x) \sin(10\pi y).$$

The boundary conditions were assumed to be insulated. The corresponding exact solution is

$$(5.1) \quad U(x, y, z, t) = \exp(-\pi^2 t) \cos(10\pi x) \sin(10\pi y) \cos(10^5 \pi z).$$

Thus, we expect positive (heating) and negative (cooling) values for the temperature in the 3D sub-microscale particle. Let $j_x = j_y = 7$ and $j_z = 20$. Define the infinity norm by

$$(5.2) \quad \text{Max Error} = \max_{i,j,k} \left| (U_{Exact})_{i,j,k}^n - U_{i,j,k}^n \right|.$$

The absolute eigenvalues of the W_N matrix is plotted in the Fig. 1. We show that the upper bound for the absolute value of W_N 's eigenvalues is 1. Thus the scheme is stable in time. In the following, Table 1 displays

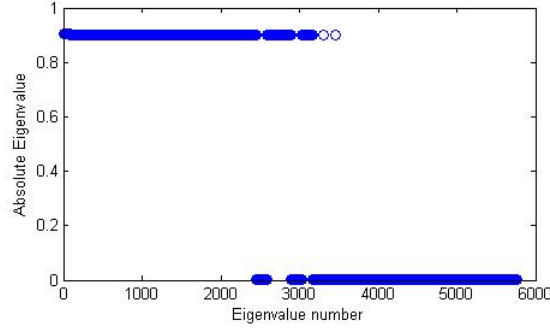


FIGURE 1. Absolute eigenvalues of W_N at Example 5.1.

the absolute of maximum error for time step $\Delta t = 0.01$ at different times. As it can be seen, the maximum error decreases down to zero against increasing time. In Table 2 the absolute error for time step $\Delta t = 0.01$ at different collocation points is given. The simulation results show a good agreement between the approximate solution and the exact solution. The 3D temperature distribution is shown in Fig. 2 for $x = 0.0703125$, $y = 0.0703125$ and $z = 7.62939453125 \times 10^{-6}$, respectively, for $\Delta t = 0.01$ at $t = 1.5$.

Example 5.2. Let 3 directions are in microscale, introduce the DPL heat equation as follows

$$(5.3) \quad \frac{\rho C_p}{\kappa} \left(\frac{\partial U}{\partial t} + \tau_q \frac{\partial^2 U}{\partial t^2} \right) = \nabla^2 U + \tau_U \frac{\partial}{\partial t} (\nabla^2 U) \frac{Q + \tau_q \partial Q / \partial t}{\kappa}.$$

TABLE 1. The Max Error for time step $\Delta t = 0.01$ in the wavelet-finite difference method for solving Eq. (5.3), in Example 5.1

t	$MaxError$	t	$MaxError$
0.5	$3.425e-04$	2	$3.022e-10$
0.8	$2.108e-05$	2.4	$6.463e-12$
1	$3.547e-06$	2.8	$1.346e-13$
1.5	$3.482e-08$	2.9	$5.099e-14$
1.8	$2.038e-09$	3	$1.929e-14$

TABLE 2. The absolute error in the wavelet-finite difference method for solving Equation (5.3), in Example 5.1

t	$x = 0.0156$ $y = 0.0625$ $z = 6.68e-6$	$x = 0.0547$ $y = 0.0156$ $z = 5.72e-6$	$x = 0.0703$ $y = 0.0156$ $z = 7.63e-6$	$x = 0.0781$ $y = 0.0156$ $z = 8.58e-6$	$x = 0.0859$ $y = 0.0156$ $z = 9.54e-6$	$x = 0.0938$ $y = 0.0547$ $z = 5.72e-6$
0.5	$9.454e-06$	$1.384e-05$	$1.251e-05$	$1.594e-05$	$2.025e-05$	$2.233e-05$
1	$1.644e-07$	$2.472e-07$	$1.632e-07$	$2.004e-07$	$2.499e-07$	$2.912e-07$
1.5	$1.762e-09$	$2.597e-09$	$1.580e-09$	$1.916e-09$	$2.375e-09$	$2.818e-09$
2	$1.614e-11$	$2.321e-11$	$1.361e-11$	$1.641e-11$	$2.027e-11$	$2.428e-11$
2.5	$1.368e-13$	$1.920e-13$	$1.104e-13$	$1.328e-13$	$1.635e-13$	$1.969e-13$
3	$1.108e-15$	$1.520e-15$	$8.632e-16$	$1.034e-15$	$1.274e-15$	$1.539e-15$

Suppose there exists a 3D Gaussian heat source

(5.4)

$$Q(x, y, z, t) = 0.94J \frac{1-R}{t_p \delta} \exp \left(-\frac{\left(x - \frac{l_x}{2}\right)^2 + \left(y - \frac{l_y}{2}\right)^2}{2r_0^2} - \frac{z}{\delta} - \frac{1.88|t - 2t_p|}{t_p} \right),$$

where $R = 0.93$, $J = 13.4 J/m^2$, $t_p = 100 fs$ ($1fs = 10^{-15}s$), $r_0 = 200 nm$ and $\delta = 15.3 nm$. Let $\kappa = 315 W/mK$, $\alpha = 1.2 \times 10^{-4}$, $\tau_q = 8.5 ps$ ($1ps = 10^{-12}s$), $\tau_U = 90 ps$, $l_x = l_y = 500 nm$, and $l_z = 100 nm$.

We use the following initial and boundary conditions

$$U(x, y, z, 0) = 300K, \quad \frac{\partial U}{\partial t}(x, y, z, 0) = 0.$$

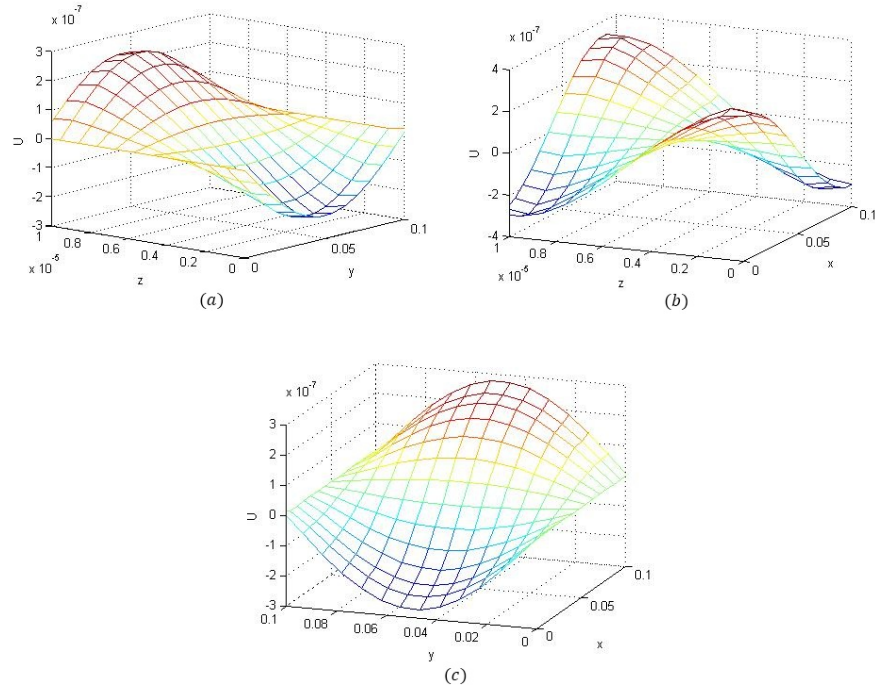
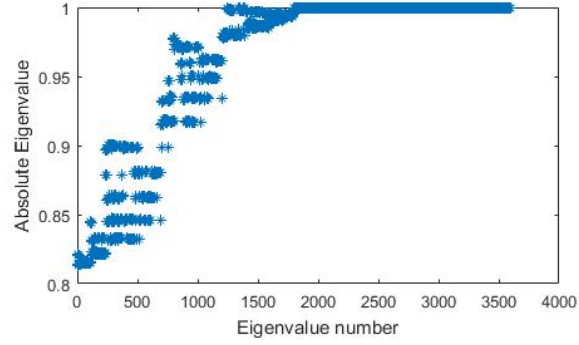
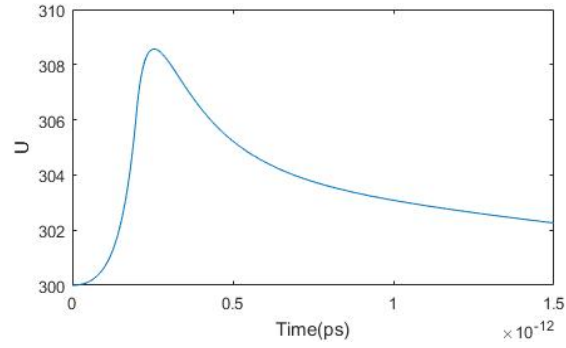
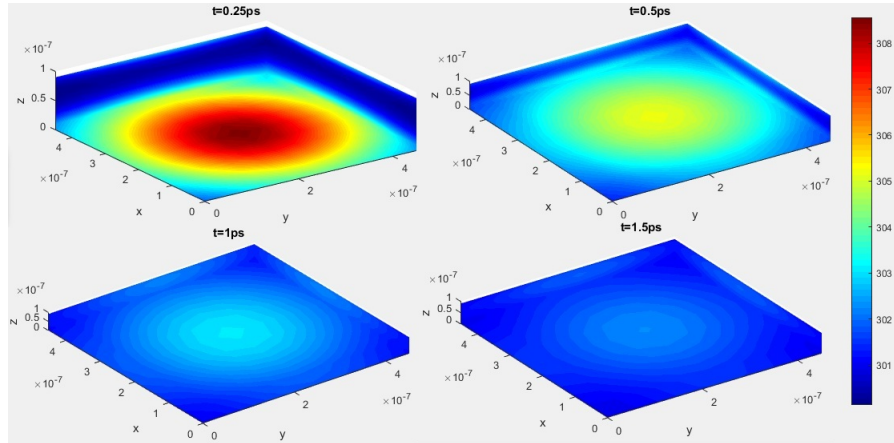


FIGURE 2. Graph of temperature distribution of Example 5.1, at $t = 1.5$ and (a) $x = 0.0703125$, (b) $y = 0.0703125$ and (c) $z = 7.62939453125 \times 10^{-6}$.

The absolute eigenvalues of W_N are plotted in the Fig. 3, that shows the upper bound for the absolute value of W_N 's eigenvalues is 1. Thus for this example, the scheme is stable in time.

In Fig.4, the temperature distribution at point $x = y = 250 \text{ nm}$ and $z = 0$, is given. This shows that, in the center of the particle, by increasing the time, the temperature decreases to $300^\circ K$. The 3D temperature distribution is shown in Fig. 5 for different times. The simulation results show that at the first time, since we use 3D Gaussian heat source, the center of particle is warm and by increasing time the temperature decreases to $300^\circ K$.

FIGURE 3. Absolute eigenvalues of W_N in Example 5.2.FIGURE 4. Graph of temperature in $x = y = 250 \text{ nm}$, and $z = 0$, using $\Delta t = 0.5 \text{ fs}$, at Example 5.2.FIGURE 5. Graph of temperature distribution of Example 5.1 at different times, using $\Delta t = 0.5 \text{ fs}$.

6. CONCLUSION

In this paper, we constructed a wavelet-finite difference approximation to the solution of the 3D time-dependent initial-boundary value problems of a microscopic heat equation using the DPL model. Eq. (5.3) with corresponding initial and boundary conditions, can be solved successfully using our proposed method. Consistency, stability and convergent of the method based on a wavelet-finite difference approximation are proved. Numerical results for temperature distribution at various times are given and the efficiency of the method is presented. The numerical results show that our method is effective.

REFERENCES

1. G. Beylkin, *Wavelets and Fast Numerical Algorithms, Lecture Notes for Short Course*, Amer. Math. Soc., Rhode Island, 1993.
2. G. Beylkin and N. Saito, *Wavelets, their autocorrelation functions, and multiresolution representation of signals*, Expanded abstract in Proceedings ICASSP-92, 4 (1992), pp. 381-384.
3. C. Canuto, M.Y. Hussaini, A. Quarteroni, and Th.A. Zang, *Spectral Methods: Fundamentals in Single Domains*, Berlin, Springer, 2006.
4. C. Canuto, M.Y. Hussaini, A. Quarteroni, and Th.A. Zang, *Spectral Methods in Fluid Dynamics*, Berlin, Springer Series in Computational Physics, 1988.
5. G. Chen, *Semi-analytical solutions for 2-D modeling of long pulsed laser heating metals with temperature dependent surface absorption*, Optik, International Journal for Light and Electron Optics, 2017.
6. R.J. Chiffell, *On the wave behavior and rate effect of thermal and thermo-mechanical waves*, M.Sc. Thesis, University of New Mexico, Albuquerque, 1994.
7. W. Dai, F. Han, and Z. Sun, *Accurate Numerical Method for Solving Dual-Phase-Lagging Equation with Temperature Jump Boundary Condition in Nano Heat Conduction*, Int. J. Heat Mass Transf., 64 (2013), pp. 966-975.
8. W. Dai and R. Nassar, *A compact finite difference scheme for solving a one-dimensional heat transport equation at the microscale*, J. Comput. Appl. Math., 132 (2001), pp. 431-441.
9. W. Dai and R. Nassar, *A compact finite difference scheme for solving a three-dimensional heat transport equation in a thin film*, Numer. Methods Partial Differ. Equ., 16 (2000), pp. 441-458.
10. W. Dai and R. Nassar, *A finite difference method for solving the heat transport equation at the microscale*, Numer. Methods Partial Differ. Equ., 15 (1999), pp. 697-708.

11. W. Dai and R. Nassar, *A finite difference scheme for solving a three-dimensional heat transport equation in a thin film with microscale thickness*, Internat. J. Numer. Methods Engrg., 50 (2001), pp. 1665-1680.
12. I. Daubechies, *Ten Lectures on Wavelets*, Soc. for Indtr. Appl. Math., Philadelphia, Number 61, 1992.
13. J. Fan and L. Wang, *Analytical theory of bioheat transport*, J. Appl. Phys., 109 (2011).
14. Z-Y. Guo and Y-S. Xu, *Non-Fourier Heat Conduction in IC Chip*, ASME J. Electron Packag., 117 (1995), pp. 174-177.
15. Z. Kalateh Bojdi and A. Askari Hemmat, *Wavelet collocation methods for solving the Pennes bioheat transfer equation*, Optik, Int. J. Light Electron Optics, 132 (2017), pp. 80-88.
16. Z. Kargar and H. Saeedi, *B-spline wavelet operational method for numerical solution of time-space fractional partial differential equations*, Int. J. Wavelets Multiresolut. Inf. Process., 15 (2017), 1750034.
17. A. Latto, L. Resnikoff, and E. Tenenbaum, *The evaluation of connection coefficients of compactly supported wavelets*, Proceedings of the French-USA Workshop on Wavelets and Turbulence, 1992, pp. 76-89.
18. A. Malek, Z. Kalateh Bojdi, and P. Nuri Niled Gobarg, *Solving Fully three-Dimensional Micros cal Dual Phase Lag Problem Using Mixed-Collocation, Finite Difference Discretization*, Trans. ASME J. Heat Transf., 134 (2012).
19. A. Malek and SH. Momeni-Masuleh, *A Mixed Collocation-Finite Difference Method for 3D Microscopic Heat Transport Problems*, J. Comput. Appl. Math., 217 (2008), pp. 137-147.
20. A. Malek and S.H. Momeni-Masuleh, *A Mixed Collocation-Finite Difference Method for 3D Microscopic Heat Transport Problems*, J. Comput. Appl. Math., 217 (2008), pp. 137-147.
21. S. Mallat, *Multiresolution approximation and wavelets*, Preprint GRASP Lab., Dept. of Computer and Information Science, Univ. of Pennsylvania, 1987.
22. T.Q. Qui and C.L. Tien, *Short-pulse laser heating on metals*, Int. J. Heat Mass Transf., 35 (1992), pp. 719-726.
23. T.Q. Qui and C.L. Tien, *Heat transfer mechanisms during short-pulse laser heating on metals*, ASME J. Heat Transf., 115 (1993), pp. 835-841.
24. G.D. Smith, *Numerical Solution of Partial Differential Equations Finite Difference Methods*, Third ed., Oxford, Oxford University Press, 1985.

25. D.Y. Tzou, *Macro to Micro Heat Transfer*, Washington, Taylor and Francis, 1996.
 26. R. Viskanta and T.L. Bergman, *Heat Transfer in Materials Processing*, Third Edition, New York, McGraw-Hill Book Company, 1998.
 27. D. Xue, *Three-dimensional simulation of the temperature field in high-power double-clad fiber laser*, *Optik, Int. J. Light Electron Optics*, (2011).
 28. J. Zhang and J.J. Zhao, *Iterative solution and finite difference approximations to 3D microscale heat transport equation*, *Math. Comput. Simulation*, 57 (2001), pp. 387-404.
-

¹DEPARTMENT OF MATHEMATICS, FACULTY OF SCIENCE AND NEW TECHNOLOGIES, GRADUATE UNIVERSITY OF ADVANCED TECHNOLOGY, KERMAN, IRAN.

E-mail address: `z.kalatehbojdi@student.kgut.ac.ir`

² DEPARTMENT OF APPLIED MATHEMATICS, FACULTY OF MATHEMATICS AND COMPUTER, SHAHID BAHONAR UNIVERSITY OF KERMAN, KERMAN, IRAN.

E-mail address: `askari@uk.ac.ir`

³ MATHEMATICS DEPARTMENT, UNIVERSITY OF MAZANDARAN, BABOLSAR, IRAN.

E-mail address: `a.tavakoli@umz.ac.ir`